Lattice-Boltzmann method combined with smoothed-profile method for particulate suspensions

Saeed Jafari,[1,2,*] Ryoichi Yamamoto,[3] and Mohamad Rahnama[2]
[1]*Department of Petroleum engineering, Shahid Bahonar University of Kerman, Kerman, Iran*
[2]*Department of Mechanical Engineering, Shahid Bahonar University of Kerman, Kerman, Iran*
[3]*Department of Chemical Engineering, Kyoto University, Kyoto 615-8510, Japan*
(Received 21 July 2010; revised manuscript received 8 December 2010; published 9 February 2011)

We developed a simulation scheme based on the coupling of the lattice-Boltzmann method with the smoothed-profile method (SPM) to predict the dynamic behavior of colloidal dispersions. The SPM provides a coupling scheme between continuum fluid dynamics and rigid-body dynamics through a smoothed profile of the fluid-particle interface. In this approach, the flow is computed on fixed Eulerian grids which are also used for the particles. Owing to the use of the same grids for simulation of fluid flow and particles, this method is highly efficient. Furthermore, an external boundary is used to impose the no-slip boundary condition at the fluid-particle interface. In addition, the operations in the present method are local; it can be easily programmed for parallel machines. The methodology is validated by comparing with previously published data.

DOI: 10.1103/PhysRevE.83.026702 PACS number(s): 02.70.−c, 82.70.Dd

I. INTRODUCTION

The flow of a dense suspension of colloidal particles is encountered in many industrial processing units. Proper investigation of fluid-particle interactions is crucial for obtaining good performance. Numerical simulations can aid in extending our understanding to more complex colloidal suspensions.

In the last two decades, the lattice-Boltzmann method (LBM) [1–4] has attracted much attention as a promising alternative for simulation of fluid flows with complex physics such as multiphase flow and multicomponent flow [5–9], simulation of particulate suspensions and colloid hydrodynamics [10–13], and adding thermal fluctuations to fluids [13–16]. The LBM is a method based on the solution of the Boltzmann equation on a lattice with a discrete velocity field. It was shown that the basic conservation equations of fluid flow (Navier-Stokes equations) can be recovered from the Boltzmann equation [17]. Solution of the Boltzmann equation provides a velocity distribution function from which macroscopic fluid properties, such as density, velocity, and pressure, can be obtained. Some advantages of using the LBM in computing fluid flow problems as compared to computational fluid dynamics (CFD) are the lack of a convective term in the Boltzmann equation and the simple pressure computation using an equation of state [2]. Moreover, the streaming-and-collision computational procedure of the LBM, which is a local operation in computation, makes it an excellent candidate for parallel computing.

The LBM has been used to simulate particles suspended in host fluids [15,16,18–20]. In some of these methods [15,16], the bounce-back rule is employed to treat the no-slip boundary condition on the fluid-particle interface, and the particle interface is represented by the boundary nodes, which are a set of midpoints of the links between two fixed grids. In these approaches, the transfer of distribution functions is used to account for the momentum transfer at the fluid-particle interface. However, with these methods, the solid boundary will not move continuously and smoothly in space; instead it will jump from one midpoint to another, causing fluctuation. Although use of a finer lattice grid with more nodes at the boundary or higher-order bounce back based on interpolations [21,22] can reduce this fluctuation, these approaches will increase the computational cost. Also, a continuous bounce-back method was developed to incorporate solid-fluid boundary conditions on length scales smaller than the grid spacing [23,24].

Another way to simulate fluid-particle interactions is to use a combination of the immersed-boundary method (IBM) and the LBM. In this kind of method [18–20], an immersed-boundary body force is introduced to capture the particle motion. In one such method, the immersed-boundary force density is worked out via a linear spring relation due to displacement between the boundary point and the computational point at the solid boundary [18]. A user-defined spring parameter may have a significant effect on the computational efficiency and accuracy. Another method computes the force density at the particle boundary by setting the velocity on the immersed Lagrangian boundary points equal to the velocity of the particle [19]. In these methods a discrete δ function is used to transform the force density from the boundary points to the flow elements. Recently, two overlapping grid systems were used [20], a regular Eulerian grid for the fluid domain and a Lagrangian for the particle domain, and the no-slip boundary condition at the solid interface was applied by adding a force density to the fluid domain to force the difference between the fluid and the solid velocity at the boundary nodes to be zero; the counterforce acting on the solid particles was used to update the position and velocity of particles based on Newtonian dynamics equations. As in previous methods, a discrete δ function was used to transform the force density from the boundary points to the Eulerian points.

To avoid complicated interpolations and transformations of the force density, a different direct forcing method is introduced based on the smoothed-profile method (SPM) [25]. It uses fixed Eulerian grids for the host fluid. It represents the particles by certain smooth body forces in the Navier-Stokes equations instead of treating the particles as boundary conditions to the fluid. The SPM solves a single set of fluid dynamics equations in the entire domain including the particle volumes, without any internal boundary conditions. A smoothly spreading interface layer is used to represent the

*jafari@alumni.iut.ac.ir

particle boundaries to give a transition from the rigid-body motion to the fluid motion. By using this simple modification, regular Cartesian coordinates can be employed for many-particle systems with any arbitrary particle shape, rather than boundary-fitted coordinates. The solid-fluid interface has a finite volume supported by multiple grid points. Thus, a round particle shape can be treated in a fixed Cartesian grid without difficulty. We do not need to consider a lot of points on the particle surface [19] or inside the particle [20]. Furthermore, the computational demands for this method include sensitivity to the number of grid points (volume of the total system); however, it is insensitive to the number of particles [25]. The common feature of using Cartesian mesh in the LBM and SPM motivates us to combine them into one efficient method. The numerical method, including the explanation of fluid-particle interaction body force, is described in the following section. Several examples are solved in Sec. III to show the accuracy and the validation of the present model. Concluding remarks are given in the last section.

II. NUMERICAL METHOD

A. Fluid flow simulation

The two-dimensional LBM is used for fluid flow simulation. In this approach, the kinetic evolution of the lattice-Boltzmann equation with the Bhatnagar-Gross-Krook (BGK) collision approximation is expressed as

$$f_\alpha(x + c_\alpha \Delta t, t + \Delta t) = f_\alpha(x,t) - \frac{1}{\tau}\left[f_\alpha(x,t) - f_\alpha^{\mathrm{eq}}(x,t)\right], \tag{1}$$

where τ is the dimensionless relaxation time, and f_α is the distribution function along the α direction. Equation (1) is a discrete finite-difference equation and is second-order accurate with respect to space and time. For the D2Q9 lattice model, that is, a model of a two-dimensional problem with nine velocities, the discrete velocities are given by $c_0 = (0,0)$; $c_\alpha = (\pm 1, 0)c$ and $(0, \pm 1)c$ for $\alpha = 1{-}4$ and $c_\alpha = (\pm 1, \pm 1)c$ for $\alpha = 5{-}8$. The streaming speed c is defined as $\Delta x/\Delta t$, where Δx and Δt are the lattice spacing and time step, respectively.

The equilibrium distribution function f_α^{eq} for the incompressible D2Q9 model is

$$f_\alpha^{\mathrm{eq}} = \omega_\alpha \rho[1 + 3(c_\alpha \cdot \mathbf{u})/c^2 + 9(c_\alpha \cdot \mathbf{u})^2/2c^4 - 3\mathbf{u}^2/2c^2], \tag{2}$$

where $\omega_0 = 4/9, \omega_\alpha = 1/9$ for $i = 1,2,3,4$ and $\omega_\alpha = 1/36$ for $i = 5,6,7,8$, and $\mathbf{u}$ is the local fluid velocity. The macroscopic variables for the fluid mass density and fluid momentum are defined by $\rho = \sum_{\alpha=1}^{8} f_\alpha$ and $\rho\,\mathbf{u} = \sum_{\alpha=1}^{8} c_\alpha f_\alpha$. By using the Chapman-Enskog procedure, the incompressible Navier-Stokes equations can be obtained from Eq. (1) with a shear viscosity $\nu = c_s^2 \Delta t(\tau - 1/2)$, where c_s is the speed of sound and $c_s^2 = c^2/3$. More details regarding the derivation of the Navier-Stokes equations from the LBM can be found elsewhere [1,2].

B. Fluid-solid interaction

A method is developed here that is based on an external boundary force [25] at the solid-fluid interface in the Navier-Stokes equation applied to the LBM to implement the no-slip boundary condition for simulation of particulate flow.

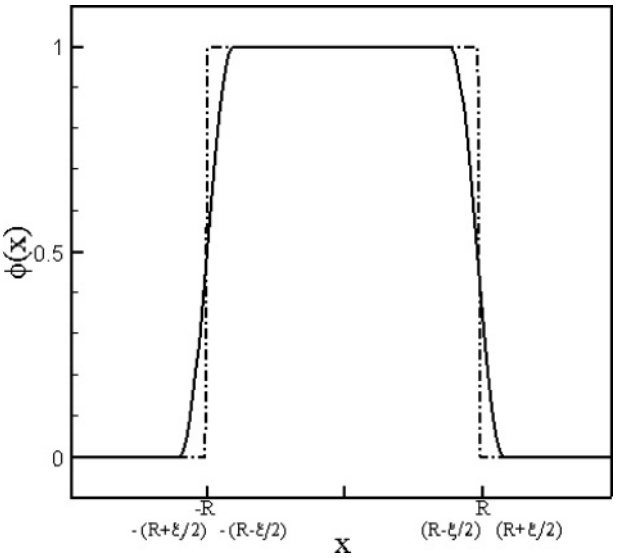

FIG. 1. An example of a smoothed profile (solid line).

In the smoothed-profile method, the surface of the colloid is treated not as a sharp interface having no thickness, but rather an interface is introduced having a width comparable to the grid spacing. The colloid density profile is defined so as to change smoothly within this finite-thickness interface.

In order to determine regions in which a colloidal particle exists, the density field is introduced:

$$\varphi(\mathbf{x},t) = \sum_{i=1}^{N_P} \varphi_i(\mathbf{x},t). \tag{3}$$

Here, $\phi_i \in [0,1]$ is the density profile of the ith particle. In the fluid regions, $\phi_i = 0$, and in particle regions, $\phi_i = 1$. Between these values its value changes continuously in the interface region of thickness ξ(Fig. 1). The functional form of ϕ is defined arbitrarily; specific examples are contained in Ref. [25]. In the present study, the following function is used:

$$\varphi_i(\mathbf{x}) = s(R - |\mathbf{x} - \mathbf{R}_i|),$$
$$s(\mathbf{x}) = \begin{cases} 0, & \mathbf{x} < -\xi/2, \\ \frac{1}{2}\sin\left(\frac{\pi \mathbf{x}}{\xi} + 1\right), & |\mathbf{x}| < \xi/2, \\ 1, & \mathbf{x} > \xi/2, \end{cases} \tag{4}$$

where R is the radius of the ith particle and $\mathbf{R}_i$ is the center position of the ith particle. The density field and velocity field of the particles at $t = t_n$ are defined using Eq. (4):

$$\varphi(\mathbf{x},t_n) = \sum_{i=1}^{N_P} s(R - |\mathbf{x} - \mathbf{R}_i(t_n)|), \tag{5}$$

$$\varphi(\mathbf{x},t_n)\mathbf{u}_P(\mathbf{x},t_n) = \sum_{i=1}^{N_P} s(R - |\mathbf{x} - \mathbf{R}_i(t_n)|) \times [\mathbf{V}_i(t_n) + \Omega_i(t_n) \times \{\mathbf{x} - \mathbf{R}_i(t_n)\}] \tag{6}$$

where $\phi\mathbf{u}_P$ is the velocity field of the particles. In the SPM, time evolution is computed for $\{\mathbf{R}_i, \mathbf{V}_i, \boldsymbol{\Omega}_i\}$ $(i = 1, \ldots, N_P)$, which are the position, translational velocity, and angular

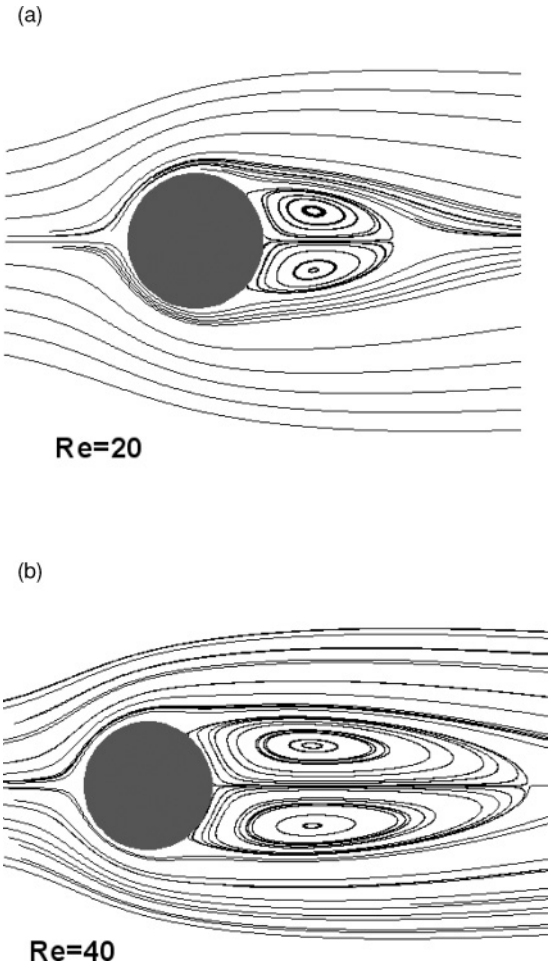

FIG. 2. Streamlines of the flow around a circular cylinder at Re = 20 and 40.

velocity of the ith particle, respectively, and $N_P$is the number of particles. Let the position, velocity, and angular velocity of the colloidal particles $\{\mathbf{R}_i, \mathbf{V}_i, \mathbf{\Omega}_i\}$ $(i = 1, \ldots, N_P)$ be given at the nth discretization time t_n. From these variables, ϕ and $\phi\mathbf{u}_P$ are constructed.

The initial velocity in the fluid domain and the particles' positions and velocities are known. The fluid nodes covered by the particle must have the same velocity as the solid particle. A body force is introduced over the particle inner domain to force the fictitious fluid to satisfy the rigid-body motion constraint; this force is zero outside the particle domain.

The fluid-solid interaction force $\phi\mathbf{f}_P$ acting on the solid particle nodes is given by

$$\int_{t_n}^{t_n+\Delta t} \varphi\,(\mathbf{x},t_n)\mathbf{f}_P(\mathbf{x},t_n)ds = \varphi(\mathbf{x},t_n)[\mathbf{u}_P(\mathbf{x},t_n) - \mathbf{u}(\mathbf{x},t_n)]. \tag{7}$$

In the above equation, $\mathbf{u}_P(\mathbf{x},t_n)$ and $\mathbf{u}(\mathbf{x},t_n)$ are the particle velocity and fluid velocity at $t = t_n$ and $\mathbf{x}$, respectively. The resulting force acting on the fluid boundary nodes is given by

$$\mathbf{f}_H(\mathbf{x},t_n) = -\int_{t_n}^{t_n+\Delta t} \varphi\,(\mathbf{x},t_n)\mathbf{f}_P(\mathbf{x},t_n)ds. \tag{8}$$

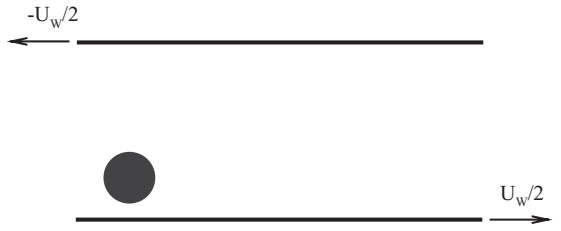

FIG. 3. A neutrally buoyant cylinder in simple shear flow.

By adding an additional term to the collision function, the fluid-solid interaction force from (8) is included in the lattice-Boltzmann equation as

$$f_\alpha(\mathbf{x}+\mathbf{c}_\alpha\Delta t, t_n+\Delta t) = f_\alpha(\mathbf{x},t_n) - \frac{1}{\tau}\left[f_\alpha(\mathbf{x},t_n) - f_\alpha^{\mathrm{eq}}(\mathbf{x},t_n)\right] + \frac{\omega_\alpha \Delta t}{c_s^2}[\mathbf{f}_H(\mathbf{x},t_n)\cdot\mathbf{c}_\alpha]. \tag{9}$$

As the particle nodes coincide with the fluid nodes, the particle-fluid interaction force is completely local and this force is zero outside the particles' domain.

The remaining steps are to update the velocity and angular velocity of particles. The force F_i^H and torque N_i^H exerted by the host fluid are obtained from the momentum conservation law. From momentum exchange during the time interval Δt, we obtain

$$\int_{t_n}^{t_n+\Delta t} \mathbf{F}_i^H\, ds = \int_{\forall_P} \rho\varphi_i(\mathbf{x},t_n)\,[\mathbf{u}(\mathbf{x},t_n) - \mathbf{u}_P(\mathbf{x},t_n)]\; d\forall_P, \tag{10}$$

$$\int_{t_n}^{t_n+\Delta t} \mathbf{N}_i^H\, ds = \int_{\forall_P} [\mathbf{x} - \mathbf{R}_i(t_n)] \times \rho\varphi_i(\mathbf{x},t_n) \times [\mathbf{u}(\mathbf{x},t_n) - \mathbf{u}_P(\mathbf{x},t_n)] d\forall_P. \tag{11}$$

Here, in order to compute F_i^H and N_i^H, the volume integral over the particle volume, $\forall_P$, is used, which is easier to compute than the surface integral [26,27].

The velocity and angular velocity of the colloidal particles are updated using this fluid drag and other forces:

$$\mathbf{V}_i(t_n+\Delta t) = \mathbf{V}_i(t_n) + M_P^{-1}\int_{t_n}^{t_n+\Delta t}\left(\mathbf{F}_i^H + \mathbf{F}_i^c + \mathbf{F}_i^{\mathrm{ext}}\right) ds, \tag{12}$$

$$\mathbf{\Omega}_i(t_n+\Delta t) = \mathbf{\Omega}_i(t_n) + \mathbf{I}_P^{-1}\int_{t_n}^{t_n+\Delta t}\left(\mathbf{N}_i^H + \mathbf{N}_i^{\mathrm{ext}}\right) ds. \tag{13}$$

In Eq. (12) F_i^c and F_i^{ext} are the collisional force on the ith particle and the external force on the ith particle, respectively, and N_i^{ext} in Eq. (13) is the external torque on the ith particle, M_P is the particle mass, and I_P is the particle moment of inertia tensor. The new particle positions are calculated by

$$\mathbf{R}_i(t_n+\Delta t) = \mathbf{R}_i(t_n) + \int_{t_n}^{t_n+\Delta t}\mathbf{V}_i ds. \tag{14}$$

The density field and velocity field of the particles for the next time step are evaluated using the updated particle positions and velocities.

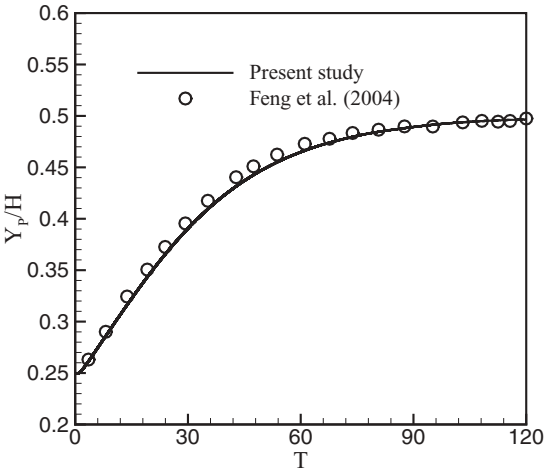

FIG. 4. Nondimensional y component of the position versus nondimensional time.

Based on the above equations, the computational scheme can be summarized as follows:

(1) At $t = t_0$, the fluid velocity and particle velocity (translational and rotational), together with the particle position (initial position when $t = t_0$) are known.

(2) The velocity field of the particles is obtained using the particle positions and velocities [Eqs. (5) and (6)].

(3) The fluid-solid interaction force $\mathbf{f}_H$ is computed using Eq. (8).

(4) The flow field is solved using the LBM [Eq. (9)].

(5) The interaction force is applied to all solid boundary nodes; the hydrodynamic force and the hydrodynamic torque acting on the particle are calculated according to Eqs. (10) and (11).

(6) The particle velocities and positions are updated [Eqs. (12), (13), and (14)]. The computations loop back to step 2.

III. RESULTS

Several problems were investigated by the present method to show its accuracy. They include flow over a circular cylinder, a neutrally buoyant cylinder in simple shear flow, two circular cylinders approaching each other in a channel, and sedimentation of two circular cylinders in a viscous fluid.

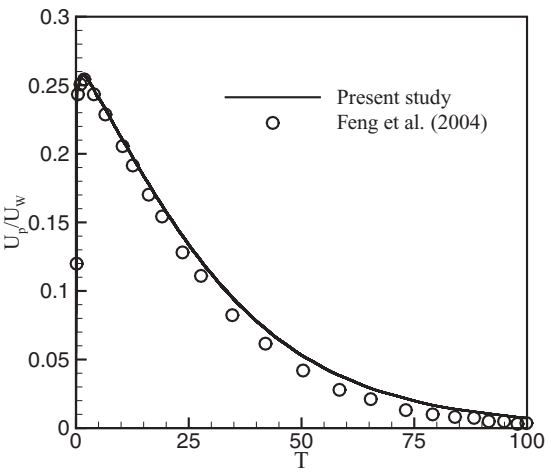

FIG. 5. Nondimensional x component of the velocity versus nondimensional time.

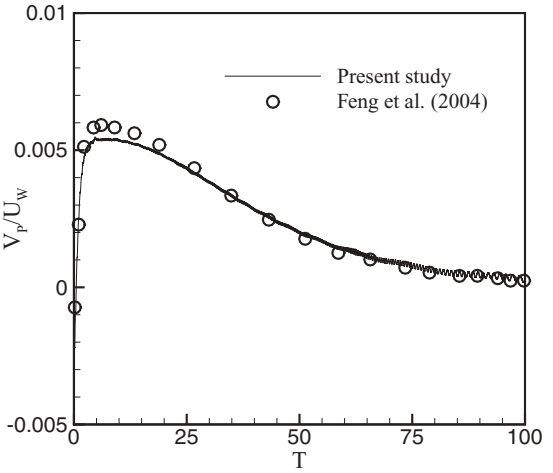

FIG. 6. Nondimensional y component of the velocity versus nondimensional time.

A. Flow over a circular cylinder

The flow over a fixed cylinder is first investigated to show the accuracy of the present method. Depending on the Reynolds number, different behavior can occur. The Reynolds number for this method is defined by

$$\mathrm{Re} = \frac{U_\infty D}{\nu},$$

where D, U_∞, and ν are the diameter of the cylinder, the free stream velocity, and the dynamic viscosity of the fluid, respectively. The simulation was performed at $\mathrm{Re} = 20$ and 40 and results were compared with previous numerical data. Figure 2 shows the computed streamlines in a domain of $L \times W = 40D \times 40D$ with a uniform mesh size of 800×800. The cylinder center is at $(2L/5, W/2)$ to decrease the effect of the outer boundary. The drag coefficient $[C_D = F_x/(0.5\rho D U_\infty^2)]$ and the length of the recirculation zone $(L_W = 2L/D)$ are compared with previous published data [19] in Table I. The present results agree well with published data. Here, in order to compute the drag force F_x, the volume integral over the particle volume is used [Eq. (10)].

B. A neutrally buoyant cylinder in simple shear flow

A schematic diagram of a neutrally buoyant cylinder in shear flow is shown in Fig. 3. The diameter of the cylinder is D

TABLE I. Comparison of the results of the present study with the results of the previous study of Niu *et al.* [19].

Reynolds number	Method	C_D	L_W
20	Present study	2.112	1.914
	Niu *et al.* [19]	2.144	1.89
40	Present study	1.598	4.81
	Niu *et al.* [19]	1.589	4.52

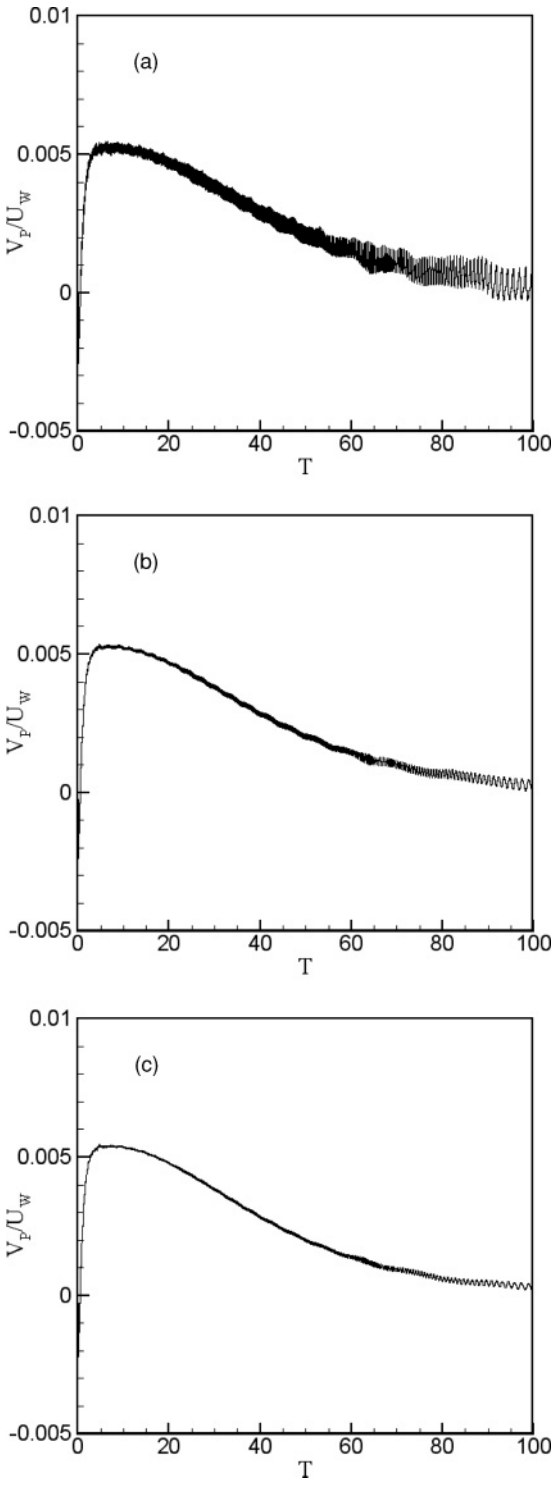

FIG. 7. Nondimensional y component of the velocity versus nondimensional time for different interface thicknesses (a) $\xi = 0$, (b) $\xi = \Delta x$, (c) $\xi = 2\Delta x$.

and it is positioned at rest halfway between the lower wall and the center between two parallel plates. The gap between the two parallel plates is $4D$. The upper and lower walls are moving at velocity $U_W/2$ in opposite directions. The computational domain is $L \times H = 100D \times 4D$, and D is selected to be 20. The fluid Reynolds number is $\mathrm{Re} = U_W H/\nu = 40$. The trajectory of the particle in the Y direction is compared with

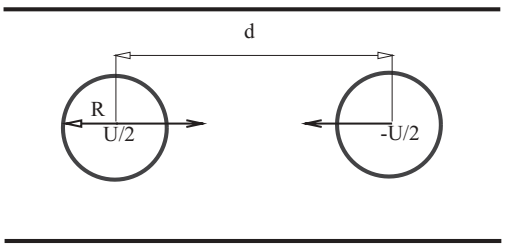

FIG. 8. Two approaching circular cylinders in a channel.

previous numerical results (Fig. 4) and shows good agreement. Figures 5 and 6 show the comparison of two components of the particle velocity obtained in the current study and in previous work [18] and perfect agreement is observed. In order to show the effect of interface thickness on the results, the upward velocity for different interface thicknesses is shown in Fig. 7. It is observed that using the smoothed-profile method reduces the small fluctuations.

C. Two circular cylinders in a channel

Results of the simulation of two circular cylinders in a channel (Fig. 8) approaching each other are presented in Fig. 9. The computational domain is $2L \times L$, and the radius of the circular cylinder is $0.2875L$. Figure 9 displays the nondimensional normal force between two cylinders versus the nondimensional distance between them, as they approach each other with speeds $\pm U/2 = \pm 0.01$, respectively. In this figure h is defined by

$$h = d - 2R,$$

where d is the distance between the two cylinders, R is the radius of the cylinder, and C is the drag force on either cylinder when far from the other cylinder. Figure 9 shows that the ability of this method to capture lubrication effects is enhanced by using a finer mesh.

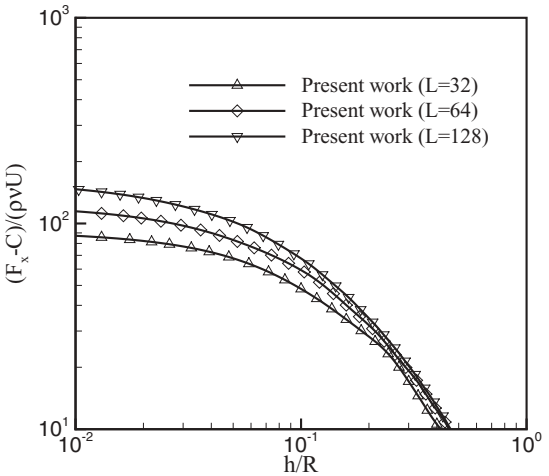

FIG. 9. Nondimensional normal force between two cylinders, approaching each other with speeds $\pm U/2 = \pm 0.01$ versus their nondimensional separation.

D. Sedimentation of two circular cylinders in a viscous fluid

In order to show the capability of the current method, the sedimentation of two circular particles in a Newtonian fluid is investigated. We have considered a channel 2 cm wide (in the x direction) and 8 cm high (in the y direction). The fluid viscosity is 0.01 g/cm s and the density is 1 g/cm^3. The particle density is 1.01 g/cm^3 and the radius is 0.1 cm. Gravity acts in the negative y direction. The simulation is started at $t = 0$ s by dropping the two particles at the center of the channel at heights of 7.2 and 6.8 cm.

To prevent the particles from overlapping with each other or the wall, artificial forces are added. In the current study the Lennard-Jones potential $\{E_{PP} = 0.4\varepsilon[(2a/R_{i,j})^{12} - (2a/R_{i,j})^6]\}$ is used, where i and j index the particles. We have

$$F_i^{P-P} = \begin{cases} 0 & R_{i,j} > 2a + \zeta, \\ 2.4\varepsilon \sum_{j=1, j\neq i}^{N_P} [2(2a/R_{i,j})^{14} - (2a/R_{i,j})^8] \frac{\mathbf{R}_i - \mathbf{R}_j}{(2a)^2}, & R_{i,j} \leqslant 2a + \zeta, \end{cases} \tag{15}$$

and

$$F_i^{P-W} = \begin{cases} 0 & R_{i,j} > a + \zeta, \\ 2.4\varepsilon \sum_{jw=1}^{jw_{\max}} [2(a/R_{i,jw})^{14} - (a/R_{i,jw})^8] \frac{\mathbf{R}_i - \mathbf{R}_{jw}}{(a)^2} & R_{i,j} \leqslant a + \zeta, \end{cases} \tag{16}$$

where $\varepsilon = a^2$,$R_{i,j} = |\mathbf{R}_i - \mathbf{R}_j|$, and $R_{i,jw} = |\mathbf{R}_i - \mathbf{R}_{jw}|$. $\mathbf{R}_{jw}$ represents the wall position and ζ is set to one lattice unit in the present work.

It is known that two particles dropped close to each other in a Newtonian fluid undergo drafting, kissing, and tumbling [18,28]. The leading particle creates a wake of low pressure, in which the trailing particle is caught, thus making it fall faster than the leading one; this stage is called drafting. Then the trailing particle with increased speed induces a kissing contact with the leading one in which the two particles form a long body with the center line along the stream. This state, which is called kissing, is unstable, and will be broken down eventually; after that the particles tumble.

Figures 10 and 11 show the plots of instantaneous vertical and horizontal positions of the two particles. The previous numerical results [18] are also included and their comparison confirms the accuracy of the present work. These figures illustrate that the results are in good agreement with the kissing of particles. It is known that the tumbling phenomenon is a realization of instability and different modes of tumbling have been reported in previous work [18,28].

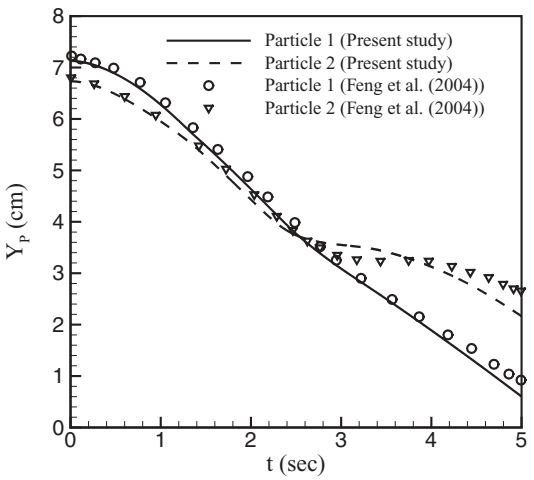

FIG. 10. Plot of instantaneous vertical positions of the two particles.

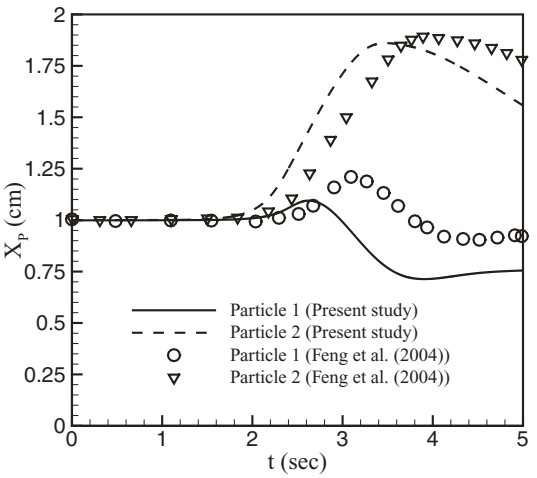

FIG. 11. Plot of instantaneous horizontal positions of the two particles.

IV. SUMMARY

The LB-SP method, which combines the smoothed-profile and the lattice-Boltzmann methods, has been proposed for simulating particle suspensions. In this method, the same computational grid is used for flow domain and particles. The no-slip boundary condition is imposed by using an external boundary force in computational nodes inside the particles. The main advantage of the present method is preservation of the merits of the LBM in simulating fluid flow. The LB-SP method has been validated by simulating the flow over a circular cylinder, a neutrally buoyant cylinder in simple shear flow, two circular cylinders approaching each other in

a channel, and sedimentation of two circular cylinders in a viscous fluid. All of the results confirm the accuracy and efficiency of the present method and its ability to simulate fluid-particle interaction problems.

ACKNOWLEDGMENTS

S.J. would like to acknowledge Professor Takaji Inamuro and Dr. Shugo Yasuda for their useful comments and discussions.

[1] S. Succi, *The Lattice Boltzmann Equation for Fluid Dynamics and Beyond* (Oxford University Press, Oxford, 2001).
[2] S. Chen and G. Doolen, Annu. Rev. Fluid Mech. **30**, 329 (1998).
[3] D. Yu, R. Mei, L. S. Luo, and W. Shyy, Prog. Aerosp. Sci. **39**, 329 (2003).
[4] C. K. Aidun and J. R. Clausen, Annu. Rev. Fluid Mech. **42**, 439 (2010).
[5] X. Shan and H. Chen, Phys. Rev. E **47**, 1815 (1993).
[6] M. R. Swift, W. R. Osborn, and J. M. Yeomans, Phys. Rev. Lett. **75**, 830 (1995).
[7] T. Inamuro, T. Ogata, S. Tajima, and N. Konishi, J. Comput. Phys. **198**, 628 (2004).
[8] A. G. Yiotis, J. Psihogios, M. E. Kainourgiakis, A. Papaioannou, and A. K. Stubos, Colloids Surf. A **300**, 35 (2007).
[9] H. Huanga and X. Y. Lu, Phys. Fluids **21**, 092104 (2009).
[10] M. Cates, K. Stratford, R. Adhikari, P. Stansell, J. Desplat, I. Pagonabarraga, and A. Wagner, J. Phys. Condens. Matter **16**, 3903 (2004).
[11] K. Stratford, R. Adhikari, I. Pagonabarraga, and J. Desplat, J. Stat. Phys. **121**, 163 (2005).
[12] R. W. Nash, R. Adhikari, and M. E. Cates, Phys. Rev. E **77**, 026709 (2008).
[13] A. J. C. Ladd and R. Verberg, J. Stat. Phys. **104**, 1191 (2001).
[14] R. Adhikari, K. Stratford, A. J. Wagner, and M. E. Cates, Eur. Phys. Lett. **71**, 473 (2005).
[15] A. J. C. Ladd, J. Fluid Mech. **271**, 285 (1994).
[16] A. J. C. Ladd, J. Fluid Mech. **271**, 311 (1994).
[17] Y. H. Qian, D. D'Humiéres, and P. Lallemand, Eur. Phys. Lett. **17**, 479 (1992).
[18] Z. G. Feng and E. E. Michaelides, J. Comput. Phys. **195**, 602 (2004).
[19] X. D. Niu, C. Shu, Y. T. Chew, and Y. A. Peng, Phys. Lett. A **354**, 173 (2006).
[20] J. Wu and C. K. Aidun, Int. J. Numer. Meth. Fluids. **62**, 765 (2010).
[21] R. Mei, L. S. Luo, and W. Shyy, J. Comput. Phys. **155**, 307 (1999).
[22] M. Bouzidi, D. d'Humieres, P. Lallemand, and L. S. Luo, J. Comput. Phys. **172**, 704 (2001).
[23] R. Verberg and A. J. C. Ladd, Phys. Rev. Lett. **84**, 2148 (2000).
[24] R. Verberg and A. J. C. Ladd, Phys. Rev. E **65**, 016701 (2001).
[25] Y. Nakayama and R. Yamamoto, Phys. Rev. E **71**, 036707 (2005).
[26] X. He, Q. Zou, L. S. Luo, and M. Dembo, J. Comput. Phys. **129**, 357 (1996).
[27] Q. Behrend, Phys. Rev. E **52**, 1164 (1995).
[28] N. A. Patankar, Annual Research Briefs-2001, Center for Turbulent Research, Stanford University, 2001 (unpublished).